

## Seismic reflection experiment with a drill-bit source

*Clement Kostov*

### ABSTRACT

The "seismic reflection experiment with a drill-bit source" consists of recording ambient noise during the drilling of a well by means of an array of geophones laid on the earth's surface. Goals of the experiment are to estimate acoustic velocities, locate the drill bit and reflectors, and image the subsurface similarly to conventional surface seismic or VSP surveys. Two challenges in processing data from this novel experiment are the separation of weak drill-bit signal from strong, spatially coherent sources of noise, such as mechanical equipment or refracted waves, and the signature deconvolution that compresses a long waveform into an impulse.

To obtain a section comparable to data from a VSP experiment, I apply a processing sequence that includes the attenuation of coherent noise by dip-filtering, the estimation of the drill-bit signature, the cross-correlation with the estimated signature, and the stack along offset after normal-moveout (NMO) correction. A stacked section for one depth interval shows an event that is continuous with depth and has the expected time-delay and moveout for a signal reflected at about 200 meters below the drill-bit.

An alternate processing sequence, not yet tested on the field data, would replace several of the stacking estimates with optimal least-squares estimates. In particular, the drill-bit signature could be estimated by solving a constrained multichannel least-squares problem. An efficient time-adaptive implementation of this algorithm, whereby the signature is estimated from a sliding window of data, can be achieved in the time-offset domain by applying Givens rotations.

### INTRODUCTION

During the drilling of a well, the impacts of the drill-bit on the rock generate acoustic waves. Part of these waves propagate as body waves to the earth surface,

carrying information about subsurface velocities, drill-bit location and reflectors. In addition to body waves generated by the drill-bit, geophones on the surface record noise from the engines on the drilling platform, from surface waves, and from waves scattered at impedance contrasts along the borehole.

To image the subsurface from records of ambient noise during drilling, two challenges have to be overcome – the separation of wavefields corresponding to different sources, and the signature deconvolution that compresses the long signal from the drill-bit source into an impulse.

When a record of the drill-bit signal is available, signature deconvolution, or simply cross-correlation can be applied to the data. Signature deconvolution reduces the volume of data, simulating an experiment with an impulsive source, and attenuates sources of noise that are incoherent *in time* with the drill-bit signal. Records of the drill-bit signal were obtained in the early 1970's by Lutz and his coworkers at Elf-Aquitaine, who attached an accelerometer to the top of the drill-string, and converted the recorded signal into a pseudo-impedance log (Lutz et al., 1972). The idea of cross-correlating accelerometer records with geophones on the ground at some distance away from the well was patented in the early 1980's (Widrow, 1986, Staron, 1988). The remarkable potential of this experiment – a transposed VSP, that provides continuous logging without interfering with the drilling operation – was demonstrated by Rector (1988) who obtained results whose quality is comparable to that of conventional VSP data.

Alternatively, body waves generated by the drill-bit could be detected and separated from noise according to their coherency *in space*. Estimation of the drill-bit signal from data recorded with a large array on the surface is discussed by Miller et al. (1988) and Kostov (1988). Two advantages of recording data with an array are the possibility of better signal/noise separation from short records in time, and the probing of a larger volume around the borehole. The processing of array data can begin either with signature deconvolution, when a pilot signal, such as an accelerometer record is available (Widrow, 1988), or with drill-bit signature estimation directly from the data (Miller et al., 1988). The data volume could be reduced by stacking along offset, in which case the data could be compared to a VSP, or else records from several depths could be stacked together and compared to surface seismic data.

A large field experiment to collect data with arrays of geophones during the drilling of a well was carried out by the *Osservatorio Geofisico Sperimentale* (OGS) last spring (OGS, 1988). Some parts of the data were made available to the SEP, and provided the experimental background against which I could test ideas for data processing.

My work with the OGS data thus far has been aimed at obtaining – by different approaches – estimates of velocities or reflector location that vary consistently with changes in offset along the array or depth of the drill-bit. Improved results could be achieved later by estimating the optimal least-squares parameters of a model for

the data. Since the volume of data acquired in this experiment is large, because the recording takes place over an extended period of time, methods for solving constrained least-squares problems adaptively in time are of interest both for off-line and on-line implementations.

Other important aspects of the project, not covered in the present report, include new acquisition geometries, experience with several data sets, and comparisons against surface seismic and VSP data.

The first part of the paper describes the physical and signal processing models that summarize my experience with field data and numerical modeling. Next, I describe the acquisition geometry used in the OGS experiment, and outline the pre-processing of the data. In the third part of the paper, I estimate time delays for the direct arrivals (velocity analysis) and the drill-bit signature. The data are then cross-correlated with the estimated signature and stacked along offset to obtain a section comparable to VSP data. Finally, I discuss the formulation of a constrained least-squares problem for the estimation of the drill-bit signature.

## MODELS FOR THE REFLECTION EXPERIMENT WITH A DRILL-BIT SOURCE

This section provides a qualitative background for the reflection experiment with a drill-bit source, and summarizes some of the particular features of that experiment observed on field data and in numerical simulations of wave propagation (Samec and Kostov, 1988).

### Spatially coherent sources of noise

The primary sources of acoustic energy are the drill-bit, the mechanical equipment near the drill site, and the ambient noise unrelated to the drilling operations – rivers, traffic. The waves incident on the array include direct and scattered arrivals from the primary sources. Examples of scattered waves are reflections of the drill-bit signal, reverberations in the borehole, radiation at impedance contrasts along the borehole, and refractions from the shallow layers (Figure 1).

Some spatially coherent sources of noise – traffic, mechanical equipment on the drilling platform – are uncorrelated in time with the drill-bit signal, and therefore readily recognized on the raw data. Reverberations in the borehole, on the other hand, generate noise that is well correlated in time and in space with the drill-bit signal. When primary signal and reverberations do not interfere, both can be considered as part of the signature. The moveout of waves from surface sources across a 1-D linear array may be similar to the moveout expected for the drill-bit signal when the sources are out of the plane of the array.

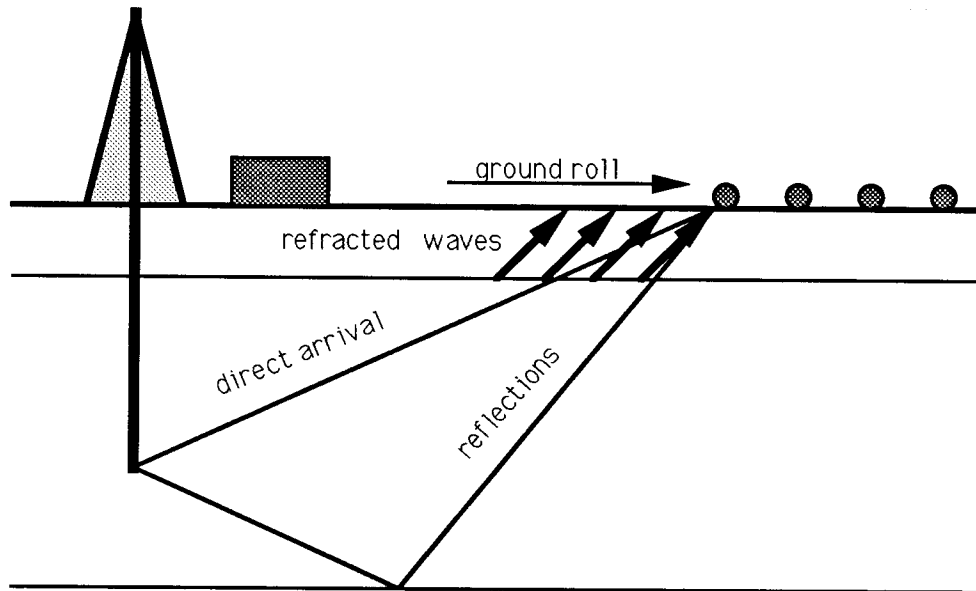


FIG. 1. Sources of acoustic energy in the seismic experiment with a drill-bit source. Primary sources include the drill-bit, pumps and generators on the drilling platform, traffic. The shallow layers act as waveguides for strong refracted waves. The drill-bit signal reverberates in the borehole and is scattered at impedance contrasts along the borehole. Part of the body waves generated by the drill-bit are reflected from layers located deeper than the well.

### Model for the drill-bit signal

A common type of drill-bit has three rotating cones, each with several crowns of about 20 teeth. As the teeth successively come in contact with the rock, the drill-bit is lifted and then impacts vertically on the rock. The periodicity and amplitude of the impulses depends on the rotational speed, on the design and state of wear of the drill-bit, and on the resistance of the rocks (Lutz et al., 1972). The drill-bit rotation rate is about 1 Hz; the symmetry of the cones and regular arrangement of the teeth excite harmonics that are integer multiples of the rotation frequency.

The drill-bit is supported by the bottom-hole assembly (BHA) and by the drill-pipes. The BHA and the drill-pipes are loosely connected steel units of rather different diameters, and therefore independent resonances occur in each unit. The periodicities of the reverberations are obtained simply from the ratio of the length of each unit to the velocity of sound in steel,  $v_s = 4.875$  Km/sec (Rector, 1988). Thus, for the BHA assembly, whose length is of the order of 100 meters, the reverberation period is about 0.04 seconds. For drill-pipes of length 700 meters the period of the reverberations is about 0.29 seconds.

## DATA FROM THE OGS EXPERIMENT

### Acquisition geometry for the OGS experiment

The data for the OGS experiment were recorded during the drilling of a 1.5 Km deep well through flat beds of sedimentary rocks, mainly sand and clay.

Five sources of data for this experiment were – (1) a surface array of geophones, (2) accelerometers on the drilling rig, (3) geophones on the drilling platform, (4) geophones buried up to 60 m deep, and (5) standard drilling logs and stacking velocities from surface seismics (OGS, 1988, Kostov, 1988).

The results in this report are obtained mainly from the vertical component geophones of the surface array, which is a single-spread linear array. The offset range was modified when the depth of the well reached 1 Km – the nearest and farthest offsets were increased respectively from 0.1 Km to 0.385 Km, and from 1.4 Km to 2.1 Km. The parameters of the seismic array are summarized in the following table, where (A) and (B) refer to the initial and latter configurations of the array.

Array Parameters	
Offset range	(A) 0.1 to 1.5 km ; (B) 0.385 to 2.1 km
Channel spacing	20 m
Number of channels	(A) 72 ; (B) 90
Groups	12 geophones per group, spaced 1.66 m apart, uniform weighting
Geophones	Vertical component, buried at 0.7 m depth
Recording Parameters	
Sampling rate in time	0.002 seconds
Length of records	10 or 25 seconds
“Shot spacing”	vertical movement of the drill bit 1 to 5 m
Number of “shot” gathers	1200
Data analyzed in this report	
(A) Depth of drill-bit 376-476 m	33 gathers, each 10 sec. long
(A) Depth of drill-bit 777-822 m	33 gathers, each 25 sec. long
(A) Depth of drill-bit 960-990 m	12 gathers, each 12 sec. long
(B) Depth of drill-bit 1291-1393 m	61 gathers, each 10 sec. long
Amount of data	300 Megabytes

To determine the frequencies excited by different engines, noise on the drilling platform was recorded with five geophones – one vertical-component and one horizontal-

component geophone near the top of the borehole, one near the trailer, another near the pumps, and a final one near the mud pits.

Three three-component geophones were buried in a shallow well at the beginning of the seismic line, at an offset of 100 m from the well. The depths of the geophones were 20 m, 40 m, and 60 m. The purpose of these geophones was to appreciate the attenuation of surface waves with depth (OGS, 1988). Another possible use of deeply buried geophones would be as a vertical antenna.

The drilling logs list several parameters at intervals of about 2-3 minutes, not necessarily related to the times when measurements were taken with the geophones. The list of parameters includes depth of the well, time of measurement, weight on bit, rotations per minute, torque, rate of penetration, flow rate, injection pressure, and volumes of mud in the pits. The power transferred to the drilling assembly is given by the product of the torque times the rotation frequency (Lutz et al., 1972). Qualitatively one would expect strong signal from the drill bit when drilling a hard formation, for which the weight on bit, torque, and rotation rates are high.

In future experiments I would recommend collecting also (1) a few gathers with a conventional, impulsive seismic source to calibrate the surface arrays for amplitude and static-delay effects, and (2) a VSP or a sonic log to check the results. The potential of this experiment for fine spatial sampling of the wavefield, either with several 1-D seismic lines or with a 2-D grid laid on the surface, could be exploited further to increase the resolution of the array and map a larger volume around the borehole.

### Preprocessing sequence

**notch filtering** The spectra of the traces are dominated by a strong peak that varies between 18 and 22 Hz, and is related to the flow-rate of the mud pump (Kostov, 1988). Thus, the first step is to suppress this dominant frequency by applying a notch filter.

**trace balancing** I apply a time-variable scaling to each trace following the recursion:

$$\begin{aligned}
 &power(0) = data^2(0) \\
 &\text{for each time } t \\
 &scaled\_data(t) = \frac{data(t)}{\sqrt{power(t)}} \\
 &power(t) = \lambda power(t-1) + (1-\lambda) data^2(t) \\
 &\text{end foreach } t.
 \end{aligned} \tag{1}$$

I also found it necessary to lowpass filter a few traces to 25 Hz; these traces were recorded without a high-cut filter being applied in the field (OGS, 1988).

**dip-filtering** A zero-phase dip-filter applied in the frequency-offset domain attenuates strong energy with a low apparent velocity of about 0.5 Km/sec and

surface waves with apparent velocity of about 1.5 Km/sec – corresponding possibly to refracted waves in the shallow layers. Figure 2 compares a window of 5 seconds of data in the offset-time domain before and after dip-filtering, while Figure 3 compares the frequency-wavenumber spectra for a window 25 seconds long.

**suppression of noise from surface sources** Some sources of noise, located on the surface, but out of the plane of the array, have hyperbolic moveouts similar to the expected moveout from the drill-bit signal. Figure 4 compares a window of a gather before and after suppression of coherent noise with a specified moveout. The moveout and signature of the noise are estimated by stacking locally along offset. Hyperbolic events with the expected moveout for the drill-bit source become apparent, when the estimated noise is subtracted from the data.

## AUTOCORRELATIONS

Autocorrelations reveal several interesting features of the data, compress the data volume, and are simple to compute. In this section, I will first identify short and long period reverberations in the borehole from displays of autocorrelations as function of the offset across the array and of the depth of the drill-bit. Then, by stacking traces along a moveout trajectory and displaying the autocorrelations of the stacked trace, I will show how stacking attenuates sources of noise.

### Reverberations in the borehole

The reverberations in the borehole introduce regularly spaced peaks in the autocorrelation of the seismic traces. Their fundamental period is given by

$$\Delta t = \frac{2 \times \text{Length}}{v_s}, \quad (2)$$

where  $v_s$  is the velocity of sound in steel ( $v_s = 4.875$  Km/sec), and “Length” is the length of the BHA or of the drill-pipes.

Figure 5 shows autocorrelations averaged over offset for three depth intervals – (1) from 376 to 476 meters, (2) from 777 to 822 meters, and (3) from 960 to 990 meters. The data vary significantly with depth, because of changes in the operating conditions of the surface equipment, and the existence of transient noise related to traffic.

The short period multiples are clearly seen for small lags of the autocorrelation. These short period multiples depend only on the length of the BHA and appear independent from offset.

Two or three bounces of long period multiples can be seen at the expected times for each depth interval – (1) 0.13 seconds, (2) 0.3 seconds, and (3) 0.33 seconds.

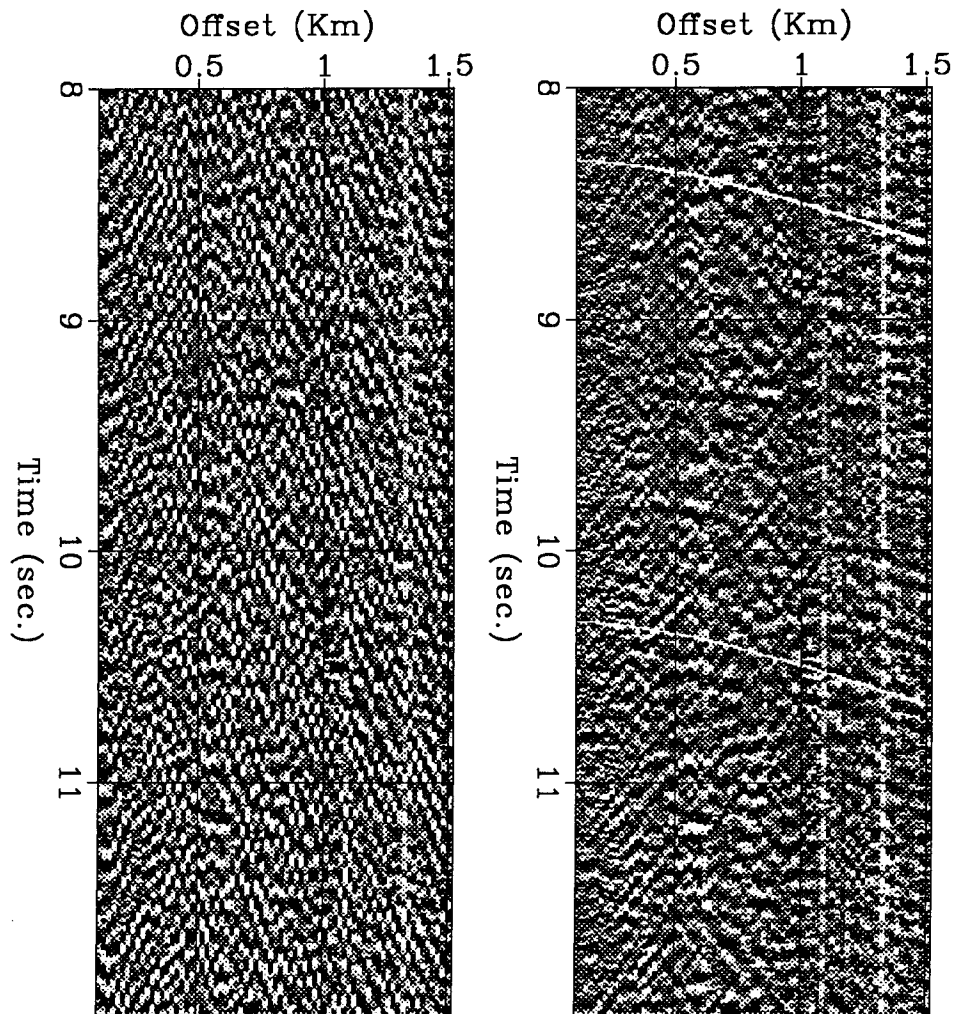


FIG. 2. Comparison of data in the offset-time domain before (left panel) and after (right panel) applying a dip-filter. The two hyperbolic lines overlaid on the right panel at 8.2 and 10.2 seconds have the moveout expected for a source at a depth of 0.8 Km/sec and for a velocity of 1.8 Km/sec. There are several hyperbolic events in the data that have similar moveouts. They are likely to be direct arrivals or multiple reverberations of the drill-bit signal.



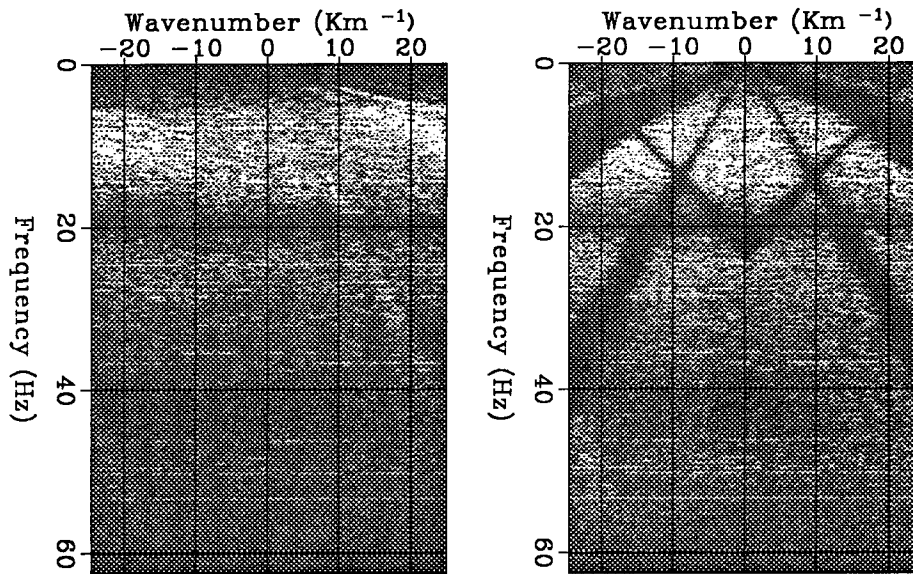


FIG. 3. Comparison of data in the wavenumber-frequency domain before (left panel) and after (right panel) applying a notch filter at about 20 Hz and dip-filtering.

The period of these multiples should increase as the length of the borehole increases. For instance, over the 45 meters of the second depth interval this increase should be 0.02 seconds – an effect measurable on the plots, and better emphasized later (Figure 11).

### Examples of sources of noise on the drilling platform

Figure 6 displays autocorrelations for a constant offset, for a constant depth, and for sensors at the surface. The strong peak at about 1 second lag on the autocorrelations of the array records (Figure 5 and Figure 6 top left and top middle) can be related to the operation of the pumps. The autocorrelation for the pilot geophone at 40 m depth also show strong noise from the pumps.

## VELOCITY ANALYSIS

To enhance the drill-bit signal, I apply the constant delays to each trace that align the direct arrivals from the drill-bit, and then sum the traces (Miller et al., 1988). In this section, I present two methods for the estimation of the time-delays of the direct arrivals.

### Hyperbola overlays

After preprocessing the data, coherent hyperbolic events become apparent (Figure 2). The time-delays that align these events can be found either by picking, or

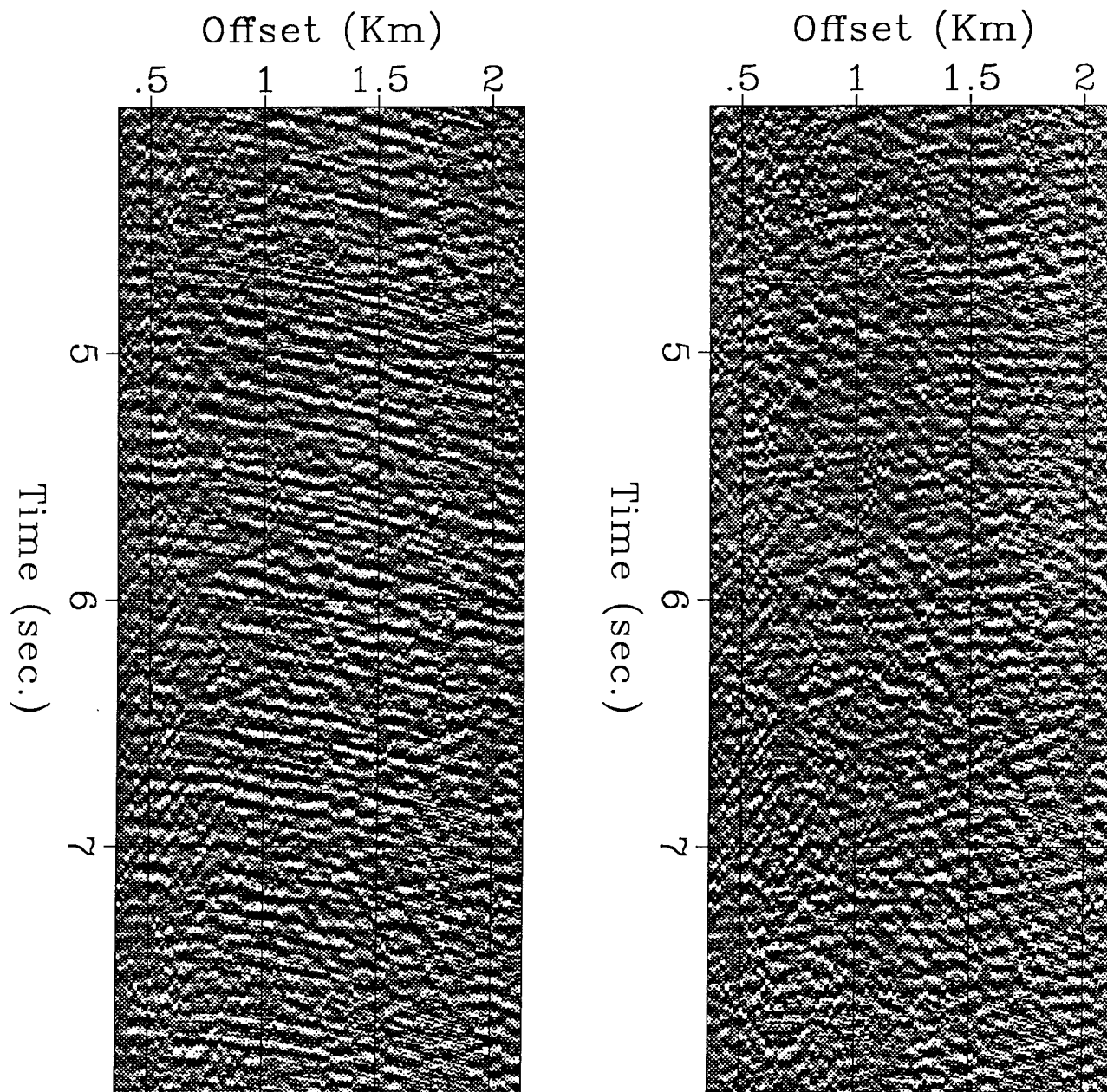


FIG. 4. (Left panel) Example of a surface source off the plane of the array that has a moveout similar to the expected moveout from the drill-bit source. (Right panel) After suppression of the dominant source of noise, hyperbolic events with moveout as expected for the drill-bit source become apparent.

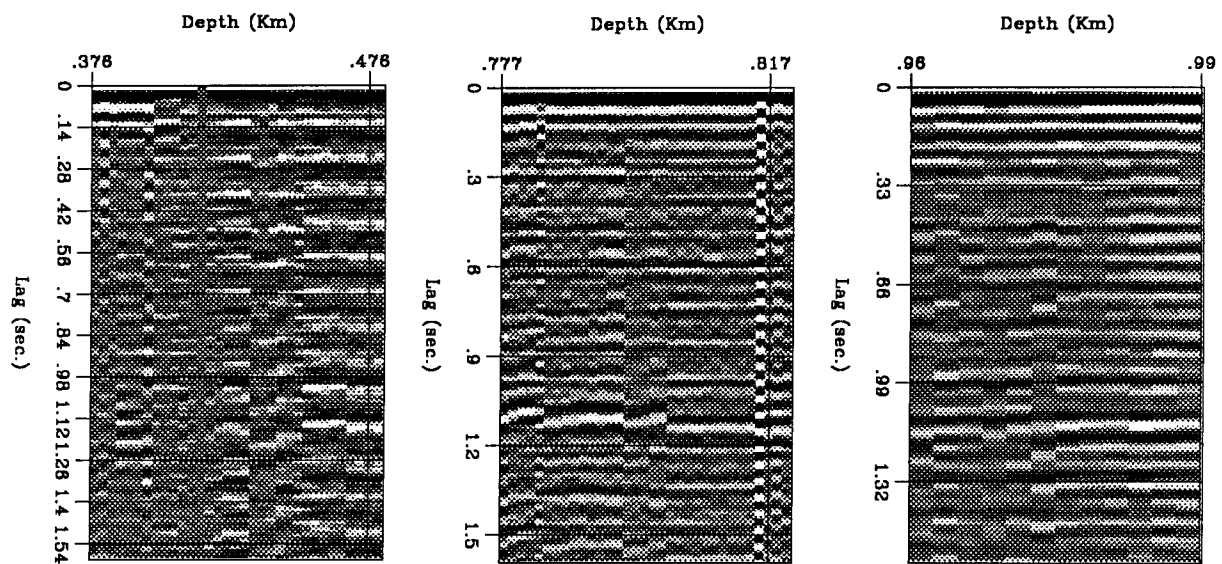


FIG. 5. Autocorrelations averaged over offset and displayed as a function of depth for three sequences of consecutive shot-gathers. Each trace in the gathers corresponds to a different position in depth of the drill-bit. Within each of the three depth intervals, the depth intervals between traces are approximately constant. The spacing of the horizontal lines on the plot is equal to the expected fundamental period for the reverberations in the drill-pipes.

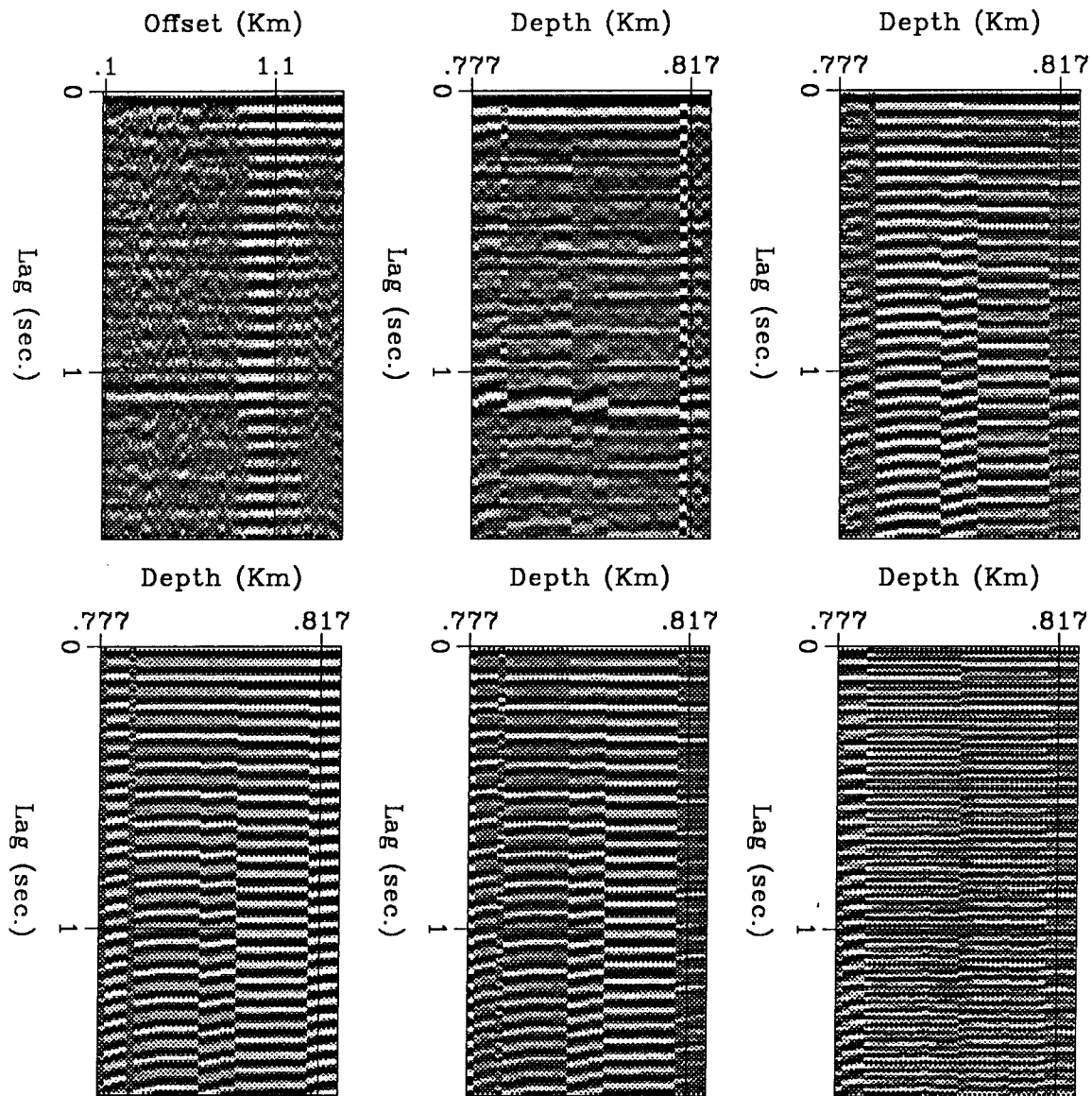


FIG. 6. A collection of autocorrelations.

Left column: (Top) Constant depth ; (Bottom) Geophone near compressors.

Middle column: (Top) Average over offset ; (Bottom) Geophone near pumps.

Right column: (Top) Geophone buried at 40 m depth ; (Bottom) Geophone near trailer .

by overlaying a hyperbola parametrized by depth of the source and velocity. Raster displays and interactive programs such as described by Claerbout (1987), Kostov and Zanzi (1988), or Dulac (1989) provide helpful tools for the picking of events on data with low signal-to-noise ratio. The interactive approach is a very powerful way of detecting weak, transient signals with an expected hyperbolic coherency. On the other hand, the estimates obtained by this approach may not be representative of the larger volume of data.

### Stacks of narrow-band spectra

Measuring the power along hyperbolic trajectories parametrized by depth of source and velocity, provides a method for velocity analysis that is complementary to the interactive picking method presented above.

The coherency spectrum  $S(z, v)$ , computed by stacking along trajectories parametrized by depth  $z$  and velocity  $v$ , is given by the following expression:

$$S(z, v) = \sum_{\omega} \left| \sum_x d(x, \omega) e^{j \frac{\omega \sqrt{x^2 + z^2}}{v}} \right|^2, \quad (3)$$

where  $\omega$  denotes frequency,  $x$  offset, and  $d(x, \omega)$  data.

An alternative expression for the contribution of a particular frequency  $\omega$  to the coherency spectrum can be given in terms of the covariance matrix of the data  $R_d(\omega)$ , defined as the outer product of the data vector  $D(\omega)$ , whose components are  $d(x, \omega)$  (Biondi and Kostov, 1989):

$$R_d(\omega) = D(\omega) D^H(\omega),$$

and

$$S(z, v) = \sum_{\omega} \mathbf{u}^H R_d(\omega) \mathbf{u}, \quad (4)$$

with the components of the steering vector  $\mathbf{u}$  being equal to  $\{e^{j \frac{\omega \sqrt{x^2 + z^2}}{v}}\}_x$ .

Figure 7 illustrates the application of this coherency analysis to a synthetic with a single broadband event. The stacking spectrum indicates maximum power for the correct values of the parameters of the hyperbolic trajectory; the peak of the stacking spectrum however is not well resolved.

When the signal is stationary in time, covariance matrices computed from several windows in time can be averaged. By modeling the data as the superposition of a few wavefronts only, it can be shown that the average covariance matrix has a particular eigenstructure. One way of reducing noise then is to replace in Equation 4 the covariance matrix of the data  $R_d(\omega)$  by a low-rank approximation (Biondi and Kostov, 1989). I computed coherency spectra by approximating the narrowband correlation matrices with rank 4 matrices. The results are displayed in Figure 8 and compared to the stacking velocities from surface seismic data (OGS, 1988). The three methods of velocity analysis – stacking velocities for surface seismic data,

stacking power on drill-bit data, and picking of events lead to the same estimated parameters for the direct arrivals – source at depth 0.8 Km and velocity of about 1.8 Km/sec.

### Correction to the stacking velocities for sources at depth

I compute the rms velocities for a source at depth by first converting stacking velocities to interval velocities, and then applying a modified Dix formula (Muir, 1987), that accounts for the observation that rays travel only once through the layers above the drill-bit, and twice through the layers below the drill-bit (Figure 9). The moveout of the direct arrivals from the drill-bit are obtained as a particular case of that formula – the source and reflector are at the same level and therefore the rms velocity is the same as for a source at the surface. Figure 10 illustrates the difference in stacking velocities for a source at the surface and for sources at depths of 0.78 and 0.82 Km. The difference in moveout resulting from a movement of the source of 35 meters is negligible, which justifies averaging coherency spectra over this range of depths.

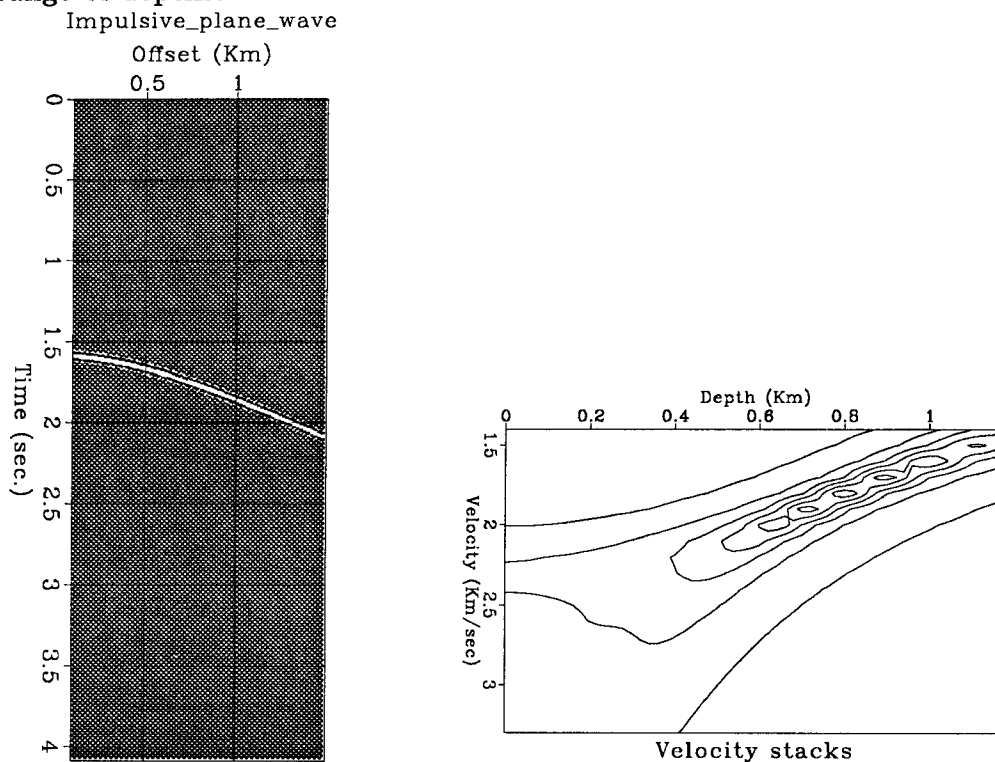


FIG. 7. (Left) A synthetic with a single hyperbolic event corresponding to a source at depth 0.8 Km and velocity of 1.8 Km/sec. (Right) A velocity spectrum obtained by stacking along hyperbolic trajectories parameterized by depth of source and velocity. The maximum occurs at the correct parameters for the hyperbolic event; there is however a family of trajectories with nearly identical stacking power.

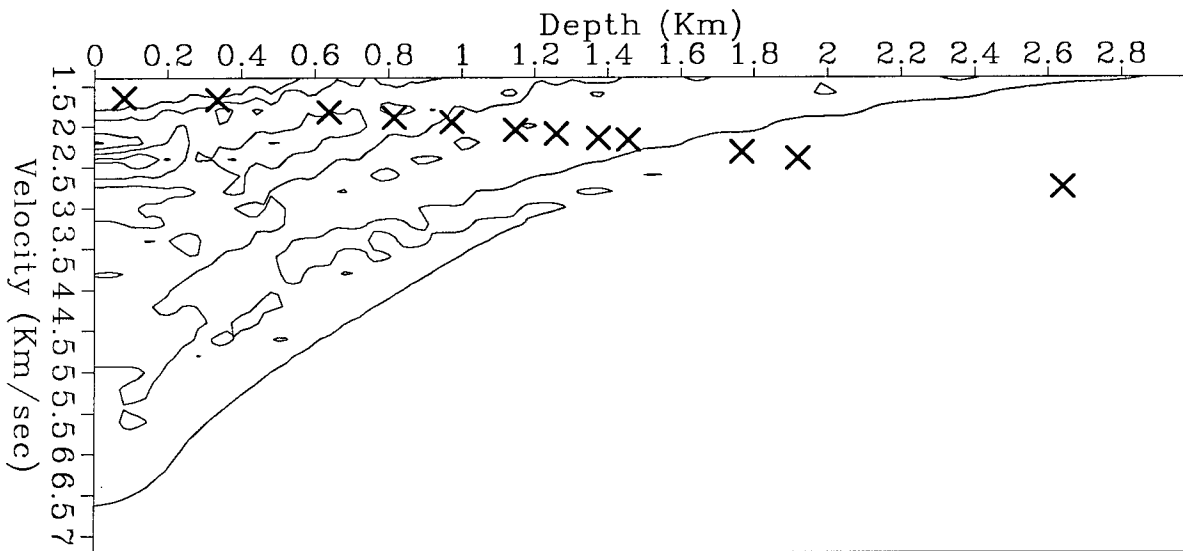


FIG. 8. Power of stack along hyperbolic trajectories parametrized by depth of the source and velocity. Crosses shows picked stacking velocities from surface seismic data. At the depth of the well, 0.8 Km, there is good agreement between the maximum power in the stack, the value given by surface seismics, and the velocities picked on the data records (Figure 2).

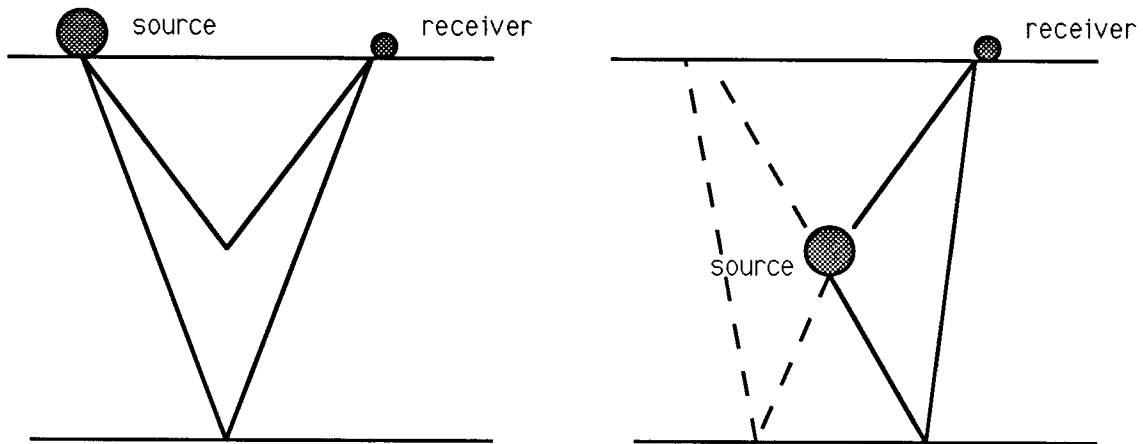


FIG. 9. Raypaths for reflections from an interface, for experiments (left) with a source at the surface and (right) a source at depth. For easier comparison, the raypaths for a source at depth have been drawn for two receivers symmetrically located on either side of the source. The raypaths for a source at the surface are "V"-shaped, while for a source at depth they are "W"-shaped. A particular case is the direct arrival from the drill-bit for which the rms velocity is the same as the rms velocity for a reflector at the same depth and a source at the surface.

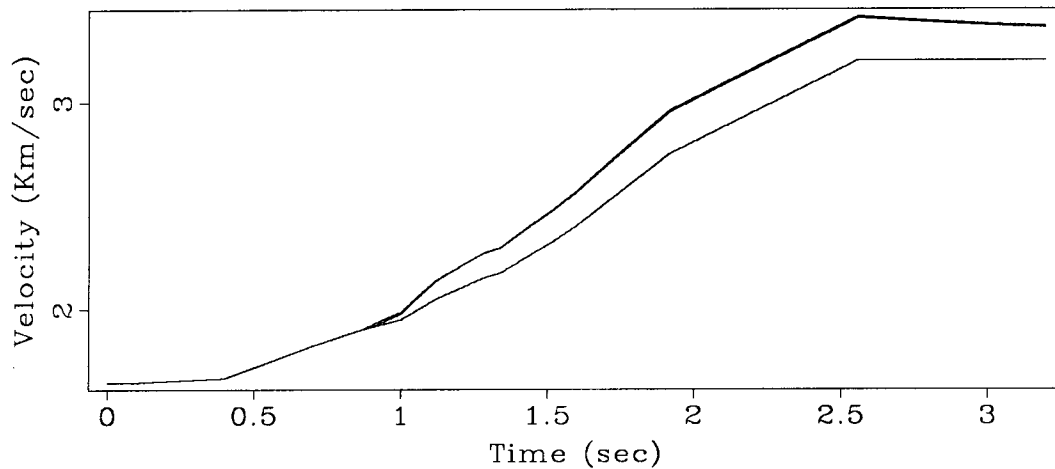


FIG. 10. Rms velocity as a function of two-way traveltime for (thin line) source at the surface and (thick line) sources at depths of 0.78 and 0.82 Km. The velocity profiles for the two sources at depth are overlapping on the scale of the plot.

### CROSS-CORRELATION AND NMO-STACK

Having determined the wavefront shape of the direct arrivals, I sum along that trajectory of coherency to estimate the drill-bit signature. Figure 11 displays the autocorrelations of the estimated signature from full and partial offset ranges as a function of the depth of the drill-bit between 777 meters and 822 meters. In comparison with the autocorrelations averaged incoherently along offset (Figure 5), the autocorrelations of the estimated signatures show weaker energy due to multiple reverberations and to surface sources of noise. One peak at about 0.3 seconds, due to a long period multiple is more continuous as a function of depth, and more visible than on Figure 5. The partial stack in the range of offsets 400 to 800 meters (Figure 11, bottom left) appears to be less contaminated by multiples and surface sources, than the autocorrelations computed from other offset ranges. I estimate the drill-bit signature from that range of offsets, and cross-correlate with the traces recorded by the surface array.

After cross-correlation, the resulting gathers should correspond to an experiment with an impulsive down-hole source. Figure 12 displays the crosscorrelations for a particular gather as a function of offset, next to a "constant offset" gather. The strongest hyperbolic event seen on the left panel, has the moveout applied to estimate the drill-bit signature. More interesting is the event at about 0.24 seconds at the near offset that has a higher apparent velocity. On the constant offset section this event has a slope, as expected for a reflection.

To attenuate noise further I applied a normal-moveout (NMO) correction with a constant velocity to the crosscorrelated gathers, and then stacked along offset.



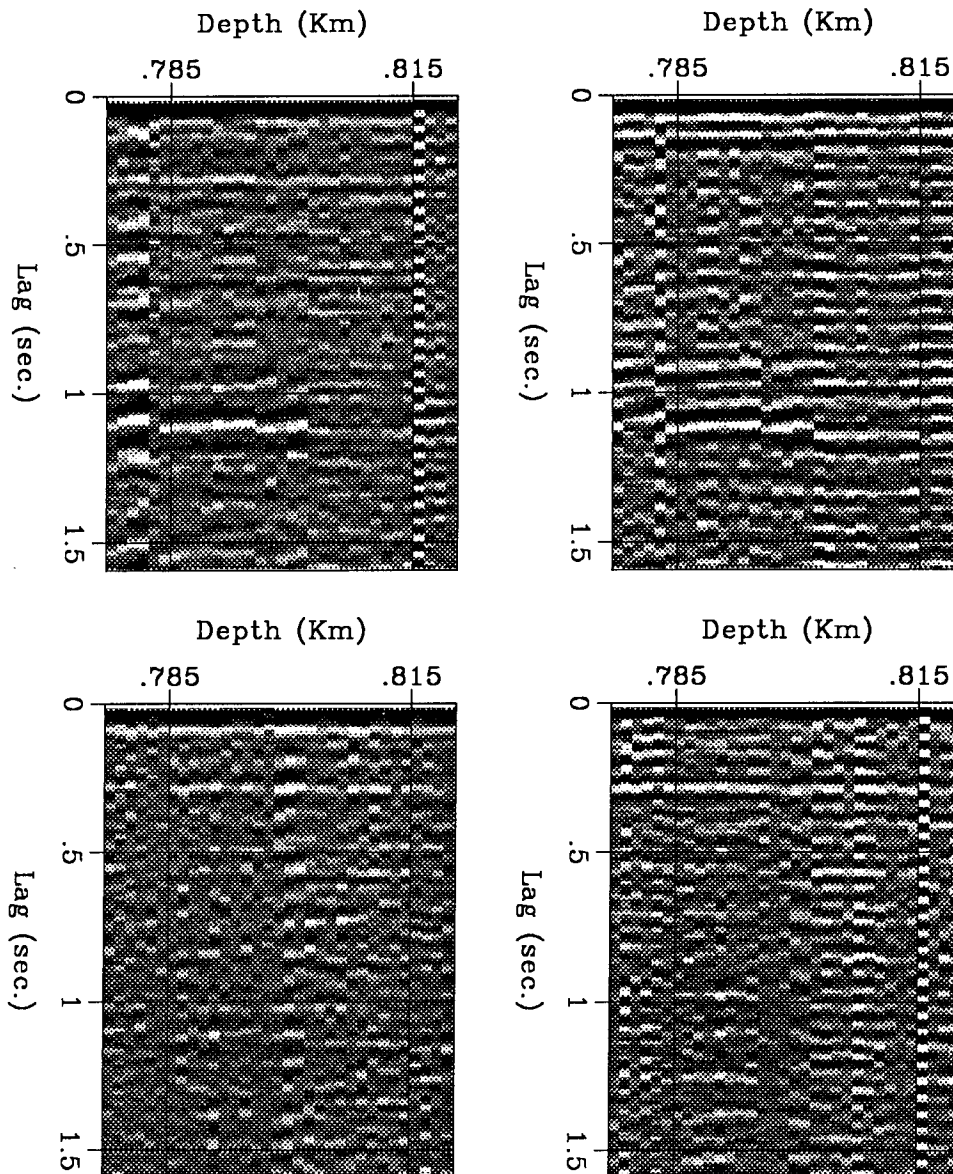


FIG. 11. Autocorrelations of traces averaged along offset after applying traveltimes delays corresponding to a hyperbolic traveltime curve parametrized by depth 0.8 Km and velocity 1.8 Km/sec.

Top: (left) all traces ; (right) near offsets .

Bottom: (left) middle offsets ; (right) far offsets.

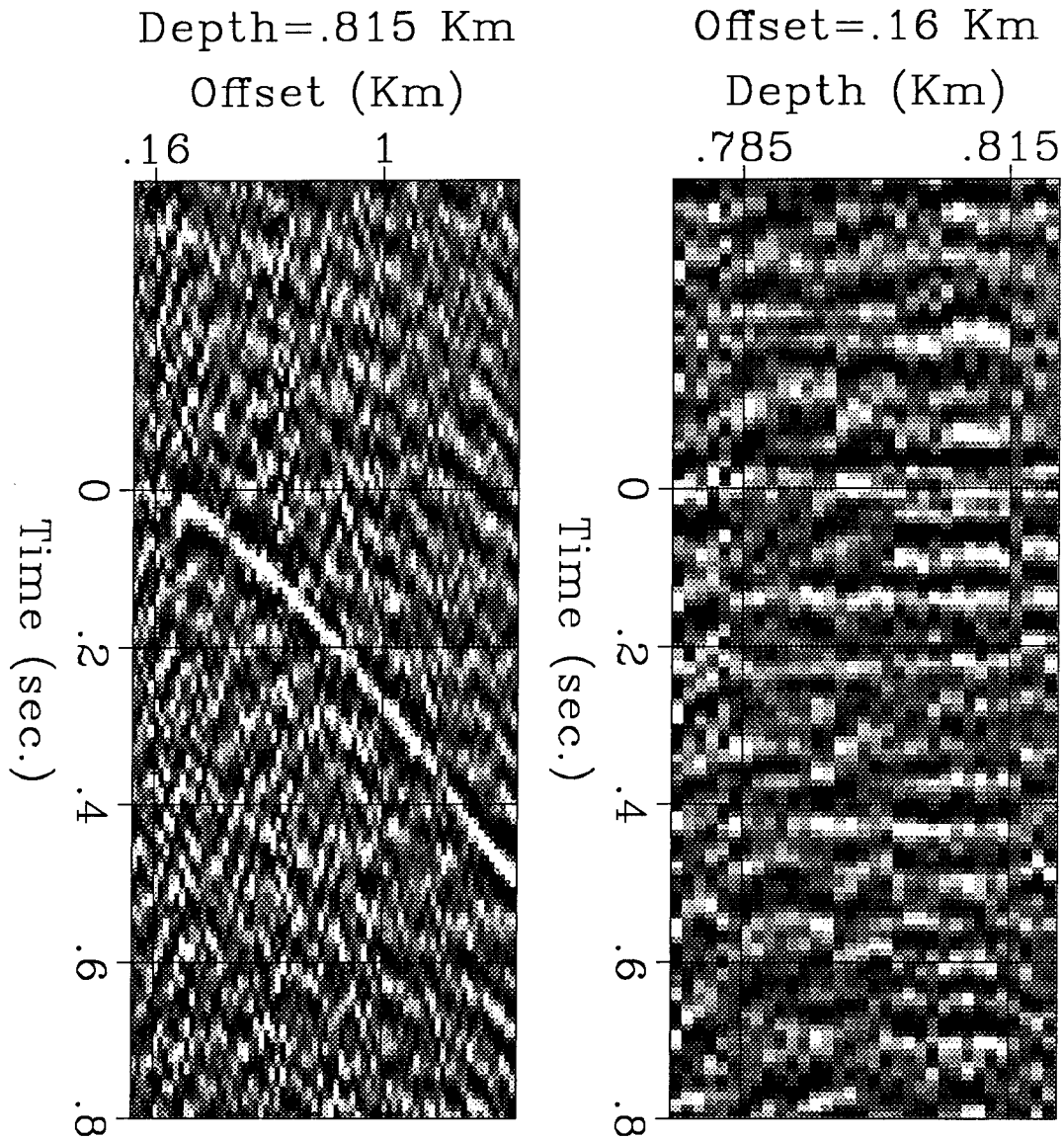


FIG. 12. (Left) Crosscorrelations between estimated signature and surface array data as function of offset. Notice the event with hyperbolic moveout at about 0.24 seconds on the near offset trace.

(Right) Crosscorrelations between estimated signature and surface array data as function of depth for a particular offset. Relate the dipping event at about 0.24 seconds to the hyperbolic event on the left panel.

Figure 13 displays the NMO-corrected and stacked traces as a function of depth. A dipping event, similar to the one seen on the constant offset section (Figure 13) has the time-delay and moveout velocity expected for a signal reflected about 200 meters ahead of the drill-bit.

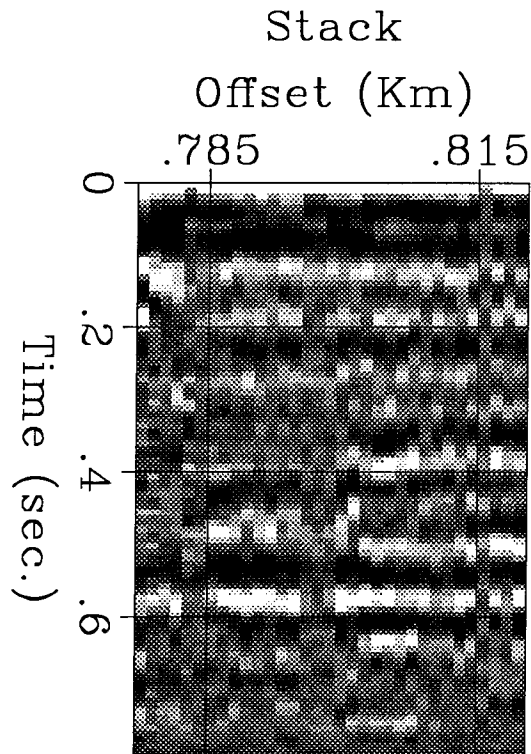


FIG. 13. Stack displayed as a function of depth and time delay with respect to the direct arrival from the drill-bit. The stack is the result of cross-correlating the data with the estimated signature, then applying NMO correction and stacking along offset. The event at about 0.24 seconds has a slope and arrival time as expected for a reflection from a layer about 200 meters ahead of the drill-bit.

## LEAST-SQUARES ESTIMATION OF THE DRILL-BIT SIGNATURE

To estimate the drill-bit signature I simply stacked along the trajectory of coherency for the direct arrivals from the drill-bit. Stacking increases the signal coherent along that trajectory, and rejects noise that has a different moveout. Stacking however yields a poor estimate when the interfering noise is strong compared to the signal, or when the difference in moveout between signal and noise is small.

In this section I outline a method that computes a convolutional filter for each trace. The convolutional filters generalize the constant scalar weights applied by the stacking operator, and provide the necessary degrees of freedom to control the attenuation response of the array.

In the presence of strong coherent noise, it is possible to estimate the moveout and signature of the dominant sources of noise, and suppress them in a manner similar to the procedure illustrated in Figure 4, where a strong source of noise is removed by a "notch" filter. This simple procedure becomes impractical to imple-

ment when the number of sources is large, and does not address the issue of the simultaneous estimation of parameters for several sources.

A different approach would be to design a filter that passes only a selected range of moveouts, and adapts the filter response depending on the data. The filter would be applied in the time-offset domain, since the drill-bit signal is broadband.

The conventional approach to this filter design problem, known also as broadband beamforming (Frost, 1972), consists in solving a least-squares problem for a set of convolutional filters – one for each trace – such that the power of the sum of filtered traces is minimized subject to a set of linear constraints. The linear constraints ensure that signals arriving within a range of moveouts and frequencies will not be attenuated. Traditionally, time-variable estimation of the filter coefficients is achieved with an LMS algorithm. The LMS algorithm solves approximately the normal equations for a least-squares problem, and its solution converges to the exact solution if certain conditions on the adaptation rate and the stationarity of the data are met (Widrow, 1986).

The solution of the least-squares problem can also be obtained by solving an overdetermined system of linear equations. The overdetermined system of equations has two subsets – a first block of equations, as many as there are data samples, expresses the minimization of the stack power, while a second block of equations introduces the linear constraints.

Consider a sliding window over the data sequence, moving along the time axis. As the reference time is increased, a sample exits the window and another enters. The corresponding changes in the linear system of equations are limited to the few equations where these two data samples occur. Givens rotations can be applied to relate the solutions of linear systems that differ by only a few equations (Golub and Van Loan, 1986, McWhirter, 1987). The resulting algorithm computes the exact solution to the least-squares problem formulated in terms of the data in a time interval.

## CONCLUSIONS

Simple processing applied to the surface array data has revealed the presence of drill-bit signal, and possibly of reflections from layers ahead of the drill-bit. Now that the signal can be “seen” on the unstacked data, several data processing approaches can be tested on these data.

Working with the field data collected by the OGS has helped me to learn a great deal about the conditions of the experiment and the characteristics of the signal and noise sources. In particular, it was confirmed that the signal from the drill-bit is an approximately periodic sequence of impulses, each impulse followed by a train of short and long period reverberations in the borehole.

Directions for future work on this project include the improvement of the estimation of signal parameters by least-squares modeling, and the continuation of field experiments with different recording geometries, and under different drilling conditions.

### ACKNOWLEDGMENTS

I thank the Osservatorio Geofisico Sperimentale in Trieste for releasing the data to the SEP, and in particular, Dr. Flavio Poletto for his assistance in preparing the tapes.

Thanks also to Francis Muir for many interesting discussions.

### REFERENCES

- Biondi, B., and Kostov, C., 1989, High-resolution velocity spectra using eigenstructure methods: to appear in *Geophysics*, **54**,no.7
- Claerbout, J. F., 1987, Interpretation with the overlay program: SEP-57, 269-300
- Dulac, J.-C., 1989, Interactive velocity analysis exercises: SEP-60.
- Frost, L., O., 1972, An algorithm for linearly constrained adaptive array processing: *IEEE Proc.* **60**, 926-935.
- Muir, F., 1987, Layered models, equivalence, and Abelian groups: SEP-56, 59-70.
- Golub, G., and Van Loan, C.F., 1984, *Matrix computations*: The Johns Hopkins University Press.
- Hale, I.D., and Claerbout, J.F., 1983, Butterworth dip-filters: *Geophysics*, **48**, 1033-1038.
- Kostov, C., 1988, Drill-bit signal: SEP-59, 11-34.
- Kostov, C., and Zanzi, L., 1988, Analysis of drill-bit data: SEP-57, 393-416.
- Lutz, J., Raynaud, M., Gstalder, S., Quichaud, C., Raynal, J., Muckelroy, J.A., 1972, Instantaneous logging based on a dynamic theory of drilling: *J. of Petr. Tech.*, JPT-3604.
- McWhirter, J., G., 1987, *Proc. SPIE*, **431**, 105-112.
- Miller, D., Haldorsen, J., Kostov, C., 1988, Methods for deconvolution of unknown source signatures from unknown waveform data: U.S. patent application 164,080.
- Osservatorio Geofisico Sperimentale (Trieste, Italy), 1988, Progetto Geobit, rapporto acquisizione dati: Osservatorio Geofisico Sperimentale.
- Rector, J. W., Marion, B. P., and Widrow, B., 1988, Use of drill-bit energy as a downhole seismic source: Presented at the 58th Ann. Internat. Mtg., Soc. Explor. Geophys.

- Samec, P., and Kostov, C., 1988, Full waveform modeling of a downhole source radiation pattern using the finite-element technique: Presented at the 58th Ann. Internat. Mtg., Soc. Explor. Geophys.
- Staron, P., et al., 1988, Method of instantaneous acoustic logging within a wellbore: U.S. patent 4,718,048; *Geophysics*, **53**, 1003-1003.
- Widrow, B., and Stearns, S.D., 1985, Adaptive signal processing: Prentice-Hall.
- Widrow, B., 1986, Seismic exploration method and apparatus for canceling interference from seismic vibration source: U.S. patent 4,556,962; *Geophysics*, **51**, 1030-1030.
- Widrow, B., 1988, Seismic processing and imaging with a drill-bit source: International patent application PCT/US87/03118.